Suffusion under different stress states

B. Oli[1*]

1 Nantes Université, École Centrale Nantes, CNRS, GeM, UMR 6183, F-44600 Saint-Nazaire, France

* bikram.oli@univ-nantes.fr

ABSTRACT

Internal erosion, caused by the movement of soil particles within a dam's embankment or foundation due to seepage, is a leading cause of dam failures worldwide. One mechanism of internal erosion is suffusion, which is the simultaneous detachment, transportation, and potential self-filtration of fine particles through pore spaces. To better understand this process, a modified triaxial bench was designed and commissioned. The device is able to apply head-controlled downward seepage flow at a specific stress state and independently control the stress state and the hydraulic loadings path. This study investigates the influence of various stress states on the initiation and development of suffusion in a gap-graded cohesionless soil using the modified triaxial erodimeter. The results show that the influence of the stress state on the erodibility classification is limited.

Keywords

Internal erosion, Suffusion, Modified triaxial bench, Stress state, Erodibility classification

RÉSUMÉ

L'érosion interne est causée par le mouvement de particules de sol à l'intérieur d'un ouvrage hydraulique en terre ou du sol de fondation sous l'action d'un écoulement. Ce processus est l'une des principales causes d'instabilités de ces ouvrages dans le monde. Un des quatre mécanismes d'érosion interne est la suffusion, qui est le processus simultané du détachement, du transport et de la potentielle filtration de particules fines au travers de l'espace poral. Pour mieux comprendre ce processus, un banc triaxial modifié a été conçu et mis en service. Le dispositif est capable d'appliquer un écoulement vertical descendant contrôlé, suivant un état de contrainte spécifique. Il donne également la possibilité de commander indépendamment l'état de contrainte et les chemins de chargement hydraulique. A l'aide de ce dispositif, une campagne expérimentale est réalisée afin d'étudier l'influence des différents états de contrainte sur l'initiation et le développement de la suffusion dans un sol pulvérulent à distribution granulométrique lacunaire. Les résultats montrent que l'influence de l'état de contrainte sur la classification d'érodibilité est limitée.

Mots clés

Erosion interne, Suffusion, Banc triaxial modifié, État de contrainte, Classification d'érodibilité

I. INTRODUCTION

Internal erosion, caused by seepage transporting soil particles within the embankment or foundation, is responsible for approximately half of all embankment dam failures (ICOLD, 2017). Suffusion, one of the four different processes of internal erosion, corresponds to the simultaneous detachment, transportation and possible self-filtration of selective fine particles which migrate through the network of pore spaces. This, in conjunction with changes in permeability, seepage velocity, gradient, porosity, density and strength, can lead to sinkholes, settlements and mechanical failure. To better understand this process, experimental tests are conducted at a laboratory scale.

The development of suffusion is commonly studied using a rigid-wall permeameter (Kenney and Lau, 1985; Moffat and Fannin, 2006; Nguyen et al., 2019; Sherard et al., 1984; Skempton and Brogan, 1994). However, this type of device does not permit the study of suffusion under tri-axial stress states. To address this, a modified triaxial device was developed to examine a suffusive soil's response under a wide range of stress states. This study investigates the influence of various stress states on the initiation and the development of suffusion for a gap-graded cohesionless soil.

II. TEST APPARATUS

The modified triaxial erodimeter can apply a controlled downward seepage flow at a specific stress-state. The device is designed to independently control the stress-state and the hydraulic loading path. The general view of the apparatus is shown in Fig 1. The top cap and the base pedestal of the triaxial cell were modified to, respectively: (i) diffuse the injected flow and (ii) collect the eroded soil particles in a downstream effluent tank. In the effluent tank, a rotational mechanism comprises 16 beakers to collect the eroded particles at different times. The discrete eroded mass measurement is favored over a continuous measurement to eliminate the pressure perturbations induced by opening and closing the downstream gate, as reported in original design of (Ke and Takahashi, 2014).

A transparent cell is used to enclose the specimen, and the confining stress is regulated while the deviatoric load is imposed on the specimen via an axial loading jack. The differential head between the inlet and the outlet of specimen is controlled by an automated upstream reservoir and a stationary downstream reservoir. The downstream mass flow rate is continuously measured to evaluate the hydraulic conductivity of the tested specimens.

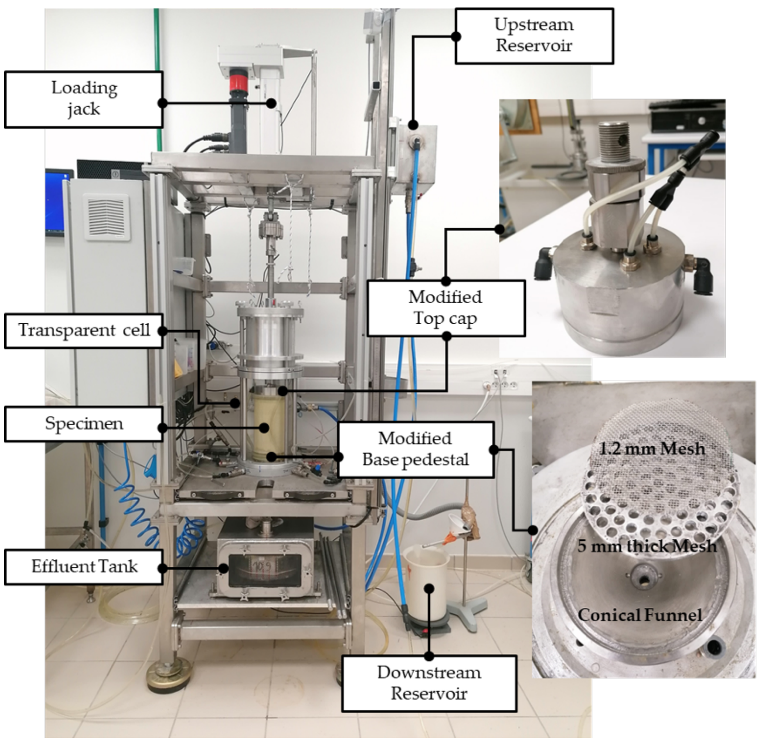

Figure 1 General view of modified triaxial bench

III. TESTED MATERIAL

A gap-graded gradation (Soil B) suspected of being prone to suffusion, is formed by mixing well-graded fine sand (P-S1) and uniformly-graded coarse gravel (P-G3), both sourced from the Sablière Palvadeau (France) quarry (see Fig 2). The tested gap-graded mixture is characterized by a gap-ratio of 2.83 and 25% of sand (P-S1), which is considered as fine fraction with respect to the coarse gravel (P-G3).

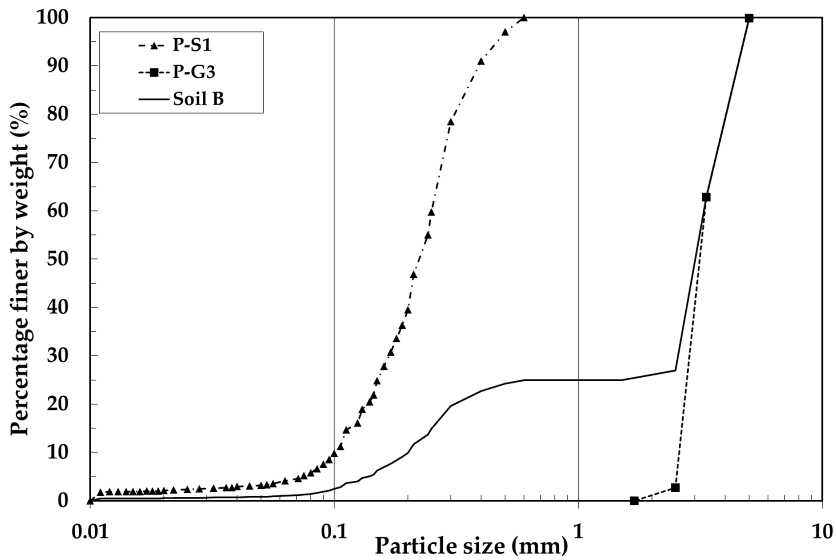

Figure 2 Reconstituted particle size distribution of tested gradation and its fractions

Based on the grain size criterion proposed by (Kenney and Lau, 1985), soil B is internally unstable (U), whereas the criterion suggested by (Chang and Zhang, 2013) classifies B as internally stable (S). Although, grain size criteria are useful as a preliminary screening tool, many soils that are neither clearly stable nor clearly unstable should be studied more closely (see Table 1) as both stress and hydraulic conditions also influence the suffusion process (Garner and Fannin, 2010).

Table 1 Characteristics of the tested gradation and potential suffusion susceptibility criteria

Tasted Gradation	P %	G_r	C_u	H/F, $_{min}$	D $(H/F)_{min}$, mm	Kenney and Lau's Criterion	Chang and Zhang's Criterion
Soil B	1.04	2.83	16.5	0.058	0.577	U	S

Note: P = percentage of particle smaller than 0.063 mm; $G_r = d_{max}/d_{min}$; d_{max} and d_{min} = maximal and minimal particle sizes characterizing the gap in the grading curve; C_u = uniformity coefficient; H = mass percentages of the grains with a size, between d and 4d, F = mass percentages of the grains with a size lower than a given particle diameter d; D $(H/F)_{min}$ = the corresponding diameter with the minimum value of ratio H/F .

III. TESTING PROCEDURE

The experiments were carried out in four phases: (i) Saturation (ii) Consolidation (iii) Erosion and (iv) Post-suffusion particle size distribution. The stress state is applied during the Consolidation phase and maintained during the Erosion phase.

For each specimen, a homogenous mixture of soil B was prepared with a 4% water content. Thereafter, the specimen (100 mm in diameter and 200 mm in height) is compacted in four layers, directly on the base pedestal with the aid of a metalic mold. The target density of 1.739 g/cm³ is achieved using the under-compaction moist tamping technique (Selig and Ladd, 1978). Afterwards, the specimen is confined with a confining pressure of 20 kPa to prevent preferential flow between the specimen and the membrane during the saturation phase. Subsequently, CO_2 is injected at a slow rate for 20 minutes and tap water is back-percolated at the rate of 0.25 mm/min to limit erosion prior to the erosion phase. Upon completion of saturation, the sample is consolidated to the target stress state. Three different values of deviatoric stress are tested with the mean effective stress being 70 kPa. Rochim et al. (2017) demonstrated that the hydraulic loading path has a significant influence on soil erodibility and multi-stage hydraulic gradient may lead to less conservative results. Therefore, suffusion is triggered by applying a controlled multi-stage hydraulic gradient (see Fig. 3). In the final phase of the test, the specimen is divided into four layers to assess the spatial variability of its post-suffusion gradation.

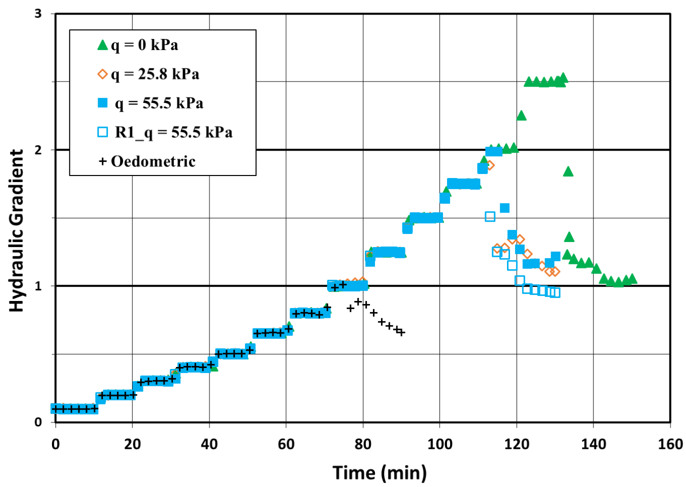

Figure 3 Multi-stage hydraulic Loading

Three tests were carried out by setting deviatoric stress to 0, 25.8 and 55.5 kPa. The maximum applied deviatoric stress corresponds to approximately 24% of the peak deviatoric stress (233 kPa) measured in the consolidated drained triaxial test. This suggests that no shear bands were formed at the applied stress level, which could have modified the flow network. To enhance the confidence of our results, the test on q = 55.5 kPa was repeated (R1_q = 55.5 kPa). Additionally, a fifth specimen was examined under oedometric conditions for comparison. Oedometric conditions involve placing the specimen in a membrane that is supported by a mould, and no confining or deviatoric stress is applied. The rest of the experimental phases are exactly similar to those mentioned for the modified triaxial erodimeter. A summary of mass lost and dry unit weight during different phases of tested specimens is presented in Table 2.

Table 2 Mass lost and dry unit weight

Tested specimen	% Fine loss during		Dry unit weight (kN/m3)	
	Saturation	Consolidation	Pre-suffusion state	Post-suffusion state
q = 0 kPa	2.79	2.66	16.83	15.90
q = 25.8 kPa	1.77	1.51	17.03	16.30
q = 55.5 kPa	1.62	2.94	17.27	16.65
R1_q = 55.5 kPa	2.54	3.37	17.05	16.44
Oedometric	1.68	/	16.99	16.33

IV.INTERPRETATIVE METHOD AND RESULTS

Marot et al. (2016) demonstrated that the hydraulic loading path can significantly alter the initiation and progression of suffusion. Therefore, the authors proposed to characterize the relevant hydraulic loading by the energy dissipated by the fluid flow E_{flow} and the soil's response by the cumulative loss dry mass m_{dry}. Loss dry mass and expended energy are two cumulative quantities that depend on the test duration. Hence, this approach requires an objective definition of the end of each suffusion test, which authors advocate to be the stabilization of the hydraulic conductivity and the decrease of the erosion rate. Over this duration, the erosion resistance index is computed by: $I_\alpha = -\log (m_{dry} / E_{flow})$ to assess the suffusion susceptibility of the tested soil.

From the time evolution of the hydraulic conductivity and the erosion rate (Fig. 4), four phases can be identified. During the first phase, hydraulic conductivity increases slightly and remains stable. The predominant process during the second phase is a self-filtration, as evidenced by the simultaneous decrease of the hydraulic conductivity and the erosion rate. The third phase is characterized by a strong increase of the erosion rate followed by a strong increase of the hydraulic conductivity. This phase is referred to as the "blow-out "event and is predominantly caused by the detachment and the transport of solid particles. In the fourth phase, the hydraulic conductivity tends to stabilize while the erosion rate decreases. This can be explained by the presence of one or more preferential flow paths created by the erosion process, leading to a final steady state. In addition, it is worth noting that under oedometric conditions, the third phase appears at a significantly lower hydraulic gradient (or cumulative energy) compared to that under triaxial stressed states. Post-suffusion particle size distributions exhibit a lower loss of fine particles, for this specimen. Indeed, oedometric conditions seem to favor a circumferential preferential flow that shortens the time required to reach the final steady state.

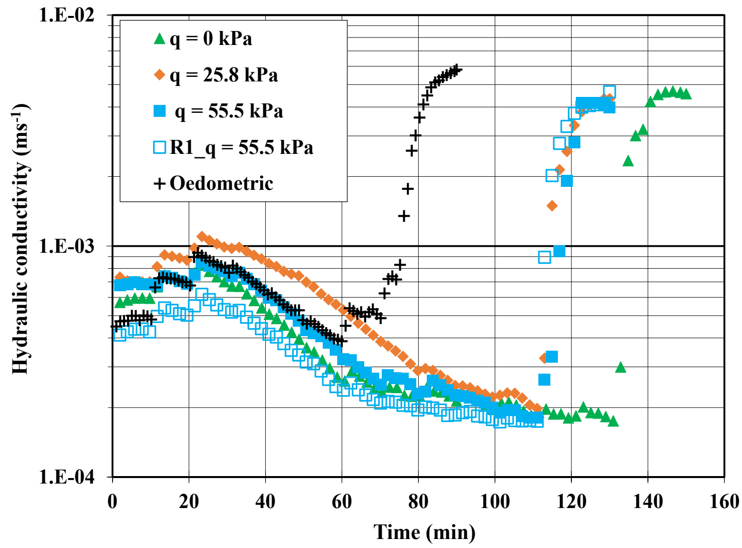

(a)

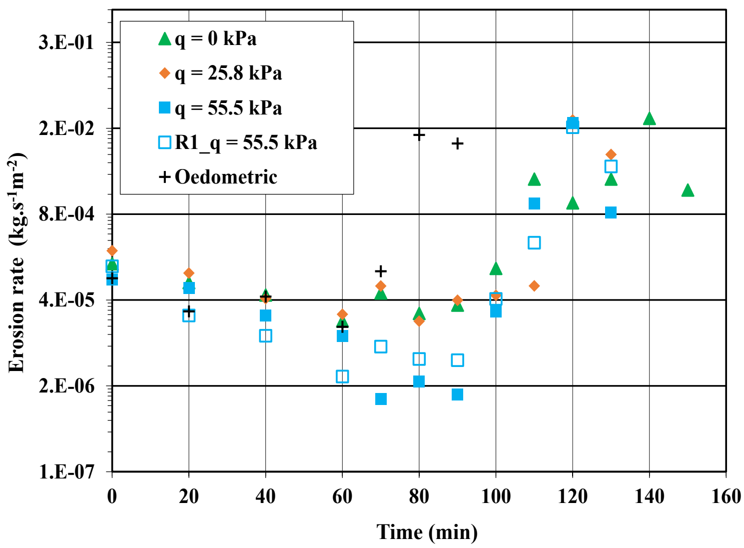

(b)

Figure 4 Time evolution of (a) the hydraulic conductivity and (b) the erosion rate

Hydraulic conductivity and erosion rate are two parameters that are measured using different methods. Hydraulic conductivity is determined by measuring the difference in hydraulic head between the top and bottom of a specimen. On the other hand, erosion rate is calculated by measuring the total mass of particles eroded during each stage of hydraulic loading, which typically lasts for 10 minutes. Detachment, transportation of particles, and partial clogging occur continuously throughout the specimen. Erosion rate provides a more immediate indication of particle detachment from the bottom of the specimen, while hydraulic conductivity decreases due to partial clogging across the specimen until sufficient hydraulic load is applied to trigger a "blow-out" event.

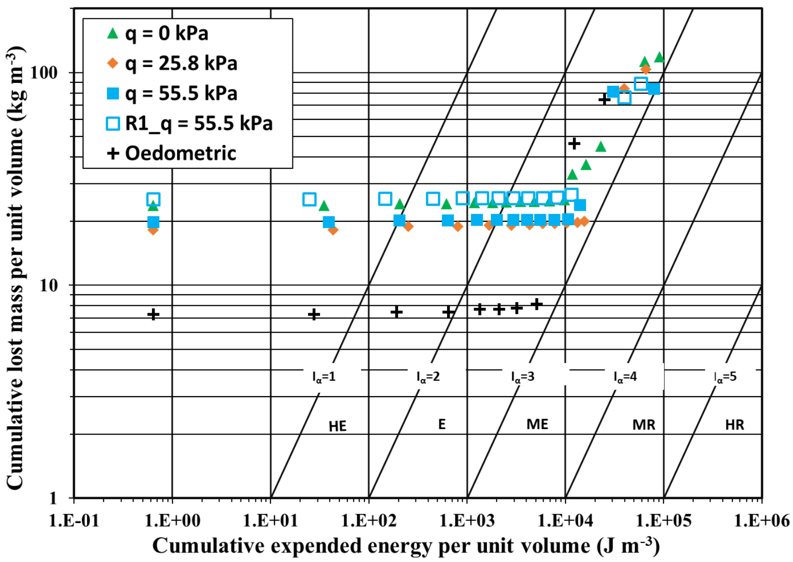

Figure 5 Erosion resistivity index classification

Interestingly, for all five performed tests, the final steady state is characterized by an erosion resistance index that lies between 2.57 and 2.91, and corresponds to the same erodible category as shown in Figure 5. A summary of key parameters determined by the test is presented in Table 3.

Table 3 Summary of tests on key parameters

Test state	i_HC	i_RE	E_MVE [kJ/m³]	Iα [SI]
q = 0 kPa	3.00	1.25	9.77	2.89
q = 25.8 kPa	2.00	1.25	15.50	2.81
q = 55.5 kPa	2.00	1.50	10.50	2.81
R1_q = 55.5 kPa	2.00	1.50	11.40	2.82
Oedometric	1.00	0.80	5.10	2.53

Note: i_HC = Hydraulic gradient corresponding to strong increase of hydraulic conductivity (blow-out event) (see Fig.4(a)); i_RE = Hydraulic gradient corresponding to the strong increase of the rate of erosion (see Fig.4(b)); E_MVE = Cumulative expended energy corresponding to the turning point of cum. lost Mass vs cum. energy (Fig.5).

V. DISCUSSION

In this section, we compare the hydraulic gradient responses under different deviatoric stress states. Using the approach outlined by Skempton and Brogan (1994), we find that the critical hydraulic gradient i_SB for all tests is 0.2 and occurs during the first phase of hydraulic conductivity. The findings suggest that, for the given soil and under multi-stage hydraulic gradient (Fig. 3), the deviatoric stress does not have any impact on the critical hydraulic gradient.

The interpretation of the test performed under oedometric conditions reveals that circumferential preferential flow paths are formed around the circumference of the specimen rather than through its body. This leads to a lower resistance in oedometric configuration as compared to triaxial stress state tests (i.e. i_HR, oedometric < i_HC, tri-axial stress state). Consequently, the occurrence of a blow-out event is shortened primarily due to the oedometric state (see Table 2). To confidently interpret the specimen's responses, based on the energy approach, it was also observed that the cumulative expended energy for the oedometric stress state is lower than that for all other triaxial stress states.

The critical hydraulic gradient associated with the turning point of erosion rate (i_RE) is consistently lower than that associated with the strong increase in hydraulic conductivity (i_HC) across all test configurations (see Table 2). This suggests that the use of the erosion rate permits to detect earlier the initiation of the blowout, then by using the hydraulic conductivity. The delay observed between these two responses is thought to be due to the interconnected processes of detachment, transportation, self-filtration, and erosion. Regardless of the different critical hydraulic gradients, it is clear that the stress state has a limited effect on the erosion resistance index (I_α) since all specimens are classified as erodible ($2 < I_\alpha < 3$, Table 2).

VI. CONCLUSION

Five suffusion tests on gap graded sandy-gravel with 25 % of sand were presented. The results illustrate the influence of the stress state on the initiation and the development of suffusion. Based on the classification proposed by Marot et al. (2016), all specimens are classified as erodible, since $2 < I_\alpha < 3$. This study suggests that the influence of the stress state on the erodibility is limited, at least for the studied soil. Complementary tests will be performed to challenge this conclusion when the percentage of sand (P-S1) is increased to 40% (i.e. when fine particles contribute more to the solid skeleton of specimen).

REFERENCES

Chang, D.S., Zhang, L.M., 2013. Extended internal stability criteria for soils under seepage. Soils Found. 53, 569–583. https://doi.org/10.1016/j.sandf.2013.06.008.

Garner, S.J., Fannin, R.J., 2010. Understanding internal erosion: a decade of research following a sinkhole event | Hydropower & Dams International.

ICOLD, 2017. Internal Erosion of Existing Dams, Levees and Dikes, and their Foundations, Bulletin 164, International Commission on Large Dams, Paris, France.

Ke, L., Takahashi, A., 2014. Triaxial erosion test for evaluation of mechanical consequences of internal erosion. Geotech. Test. J. 37, 347–364.

Kenney, T.C., Lau, D., 1985. Internal stability of granular filters. Can. Geotech. J. 22, 215–225. https://doi.org/10.1139/t85-029.

Marot, D., Rochim, A., Nguyen, H.-H., Bendahmane, F., Sibille, L., 2016. Assessing the susceptibility of gap-graded soils to internal erosion: proposition of a new experimental methodology. Nat. Hazards 83, 365–388. https://doi.org/10.1007/s11069-016-2319-8.

Moffat, R., Fannin, J., 2006. A Large Permeameter for Study of Internal Stability in Cohesionless Soils. Geotech. Test. J. 29, 100021. https://doi.org/10.1520/GTJ100021.

Nguyen, C.D., Benahmed, N., Andò, E., Sibille, L., Philippe, P., 2019. Experimental investigation of microstructural changes in soils eroded by suffusion using X-ray tomography. Acta Geotech. 14, 749–765. https://doi.org/10.1007/s11440-019-00787.

Rochim, A., Marot, D., Sibille, L., Thao Le, V., 2017. Effects of Hydraulic Loading History on Suffusion Susceptibility of Cohesionless Soils. J. Geotech. Geoenviron. Eng. 143, 04017025. https://doi.org/10.1061/(ASCE)GT.1943-5606.0001673.

Selig, E., Ladd, R., 1978. Preparing Test Specimens Using Undercompaction. Geotech. Test. J. 1, 16. https://doi.org/10.1520/GTJ10364J.

Sherard, J.L., Dunnigan, L.P., Talbot, J.R., 1984. Basic Properties of Sand and Gravel Filters. J. Geotech. Eng. 110, 684–700. https://doi.org/10.1061/(ASCE)0733-9410(1984)110:6(684).

Skempton, A.W., Brogan, J.M., 1994. Experiments on piping in sandy gravels. Géotechnique 44, 449–460. https://doi.org/10.1680/geot.1994.44.3.449.